Complexity in bacterial cell–cell communication: Quorum signal integration and subpopulation signaling in the *Bacillus subtilis* phosphorelay

Ilka B. Bischofs[a,b,1], Joshua A. Hug[c], Aiwen W. Liu[a], Denise M. Wolf[b], and Adam P. Arkin[a,b,1]

Departments of [a]Bioengineering and [c]Electrical Engineering, University of California, 311 Hildebrand Hall, MC 5230, Berkeley, CA 94704-3224; and [b]Physical Biosciences Division, Lawrence Berkeley Laboratory, 1 Cyclotron Road, MS Calvin, Berkeley, CA 94720

Edited by John Ross, Stanford University, Stanford, CA, and approved March 20, 2009 (received for review October 30, 2008)

A common form of quorum sensing in Gram-positive bacteria is mediated by peptides that act as phosphatase regulators (Phr) of receptor aspartyl phosphatases (Raps). In *Bacillus subtilis*, several Phr signals are integrated in sporulation phosphorelay signal transduction. We theoretically demonstrate that the phosphorelay can act as a computational machine performing a sensitive division operation of kinase-encoded signals by quorum-modulated Rap signals, indicative of cells computing a ''food per cell'' estimate to decide whether to enter sporulation. We predict expression from the *rapA-phrA* operon to bifurcate as relative environmental signals change in a developing population. We experimentally observe that the *rapA-phrA* operon is heterogeneously induced in sporulating microcolonies. Uninduced cells sporulate rather synchronously early on, whereas the RapA/PhrA subpopulation sporulates less synchronously throughout later stationary phase. Moreover, we show that cells sustain PhrA expression during periods of active growth. Together with the model, these findings suggest that the phosphorelay may normalize environmental signals by the size of the (sub)population actively competing for nutrients (as signaled by PhrA). Generalizing this concept, the various Phrs could facilitate subpopulation communication in dense isogenic communities to control the physiological strategies followed by differentiated subpopulations by interpreting (environmental) signals based on the spatiotemporal community structure.

heterogeneity | Phr | quorum sensing | sporulation | model

The 11 homologous *rap-phr* genes in *Bacillus subtilis* code for a family of proteins in which Rap activity is regulated by small peptides derived from the cognate *phr* gene product (Fig. 1*A*) (1). The small Phr precursor peptides are cleaved and secreted from the cell, and at least some of them accumulate in the culture supernatant (2). They are subsequently imported by Opp oligopeptide permeases into the cytoplasm where the Phr derived pentapeptides (PEP5) intracellularly inhibit the activity of their cognate Raps (3–5). Thus, PEP5s can be indicators of cell density and have been implied in facilitating cell–cell communication (2, 5–8). A subset of Raps (RapA,B,E,H) act as phosphatases that inhibit signaling through a central phosphorelay, and their activity is counteracted by their cognate PEP5s (PhrA,C,E,H). The phosphorelay plays a central role in *B. subtilis* stress response induction during stationary phase and ultimately controls sporulation induction (Fig. 1*B*) (9).

Unlike autoinducer quorum signals, where autoinducer molecules bind to a transcription factor, peptide based quorum signaling indirectly regulates transcription by controlling phosphoryl signaling (10). The presence of an autoinducer signal is typically sufficient to activate a pathway and induce a cell response (Fig. 2*A Left*). In contrast, because the Phr signal acts on a phosphatase, it instructs cells by regulating the phosphoryl flux originating from the activation of kinases that are under control of the environment (Fig. 2*A Right*). For example, it is well known that sporulation is affected by cell density. However, a high cell density alone is not sufficient to trigger spore formation unless there is a starvation signal in addition, whereas starvation alone is able to trigger sporulation, albeit at a reduced efficiency (5, 11). It therefore appears that the Rap-Phr-systems have evolved toward a mode of quorum signaling to which signal integration is essential.

It has recently been shown that even monocultures show a large degree of diversity by heterogeneous cell differentiation and population structuring (12). Stochastic population splitting has been demonstrated for a variety of stress responses including sporulation, competence, motility, extracellular matrix production, and exoenzyme synthesis (13–16). The coordinated development of specialized differentiated subpopulations implies a potential need for cell–cell signaling systems that facilitate communication among and across differentiating subpopulations. The Rap-Phr genes comprise a promising family to mediate such subpopulation signaling.

Here, we begin to explore these two aspects of Rap-Phrs in phosphorelay signaling: signal integration and subpopulation signaling. First, we develop a computational model to address the interplay of quorum and environmental signals in phosphorelay signaling and show that the signal transduction architecture supports a sensitive ratiometric integration of kinase-encoded environmental signals with respect to quorum-modulated phosphatase signals. This is indicative of a cell-density-dependent normalization of the environmental stressors such as starvation to drive downstream decision making. Within this theoretical framework, we predict a bifurcation of RapA/PhrA expression as relative environmental conditions change. We then experimentally elucidate the dynamics and fate of the previously observed subpopulation of RapA/PhrA-expressing cells (17) late into stationary phase and suggest the PhrA/RapA may be a subpopulation communication system to measure its own population size. Although the experiments do not directly test the theory, the theory aids in interpreting the importance of the experimental observations. Together, our computational and experimental results suggest a model in which phosphorelay-based decision making during starvation is based on normalizing environmental signals (such as ''food'') with respect to the size of a growing subpopulation actively competing for nutrients (''food per growing cell''). Generalizing this concept, we suggest that phosphorelay-integrated Rap-Phrs play a central role in determining and maintaining cell differentiation development by integrating (environmental) signals based on the local community structure.

Author contributions: I.B.B., D.M.W., and A.P.A. designed research; I.B.B., J.A.H., and A.W.L. performed research; I.B.B. contributed new reagents/analytic tools; I.B.B., J.A.H., and A.P.A. analyzed data; and I.B.B. and A.P.A. wrote the paper.

The authors declare no conflict of interest.

This article is a PNAS Direct Submission.

[1]To whom correspondence may be addressed at: Physical Biosciences Division, Lawrence Berkeley Laboratory, 1 Cyclotron Road, MS Calvin, Berkeley, CA 94720. E-mail: aparkin@lbl.gov or ibbischofs@lbl.gov.

This article contains supporting information online at www.pnas.org/cgi/content/full/0810878106/DCSupplemental.

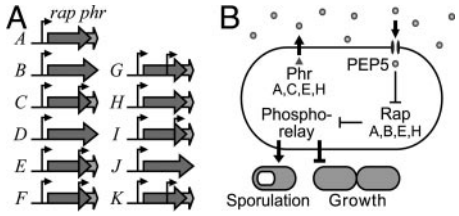

Fig. 1. Quorum signaling in *B. subtilis*. (*A*) Overview of *rap-phr* gene cassettes found in the chromosome (1). Dark arrows denote *rap* and light arrows *phr*. Bent arrows indicate start sites of transcription. (*B*) Schematic model of Rap-Phr signal integration in phosphorelay signal transduction explained in more detail in the introduction.

This implies that the various Phr-Rap systems could serve as cell–cell communication among differentiated subpopulations in dense isogenic communities, e.g., in biofilms (12) or fruiting bodies (18), where environmental signals need to be interpreted based on the spatiotemporal community structure.

Results

Signal Integration in a Conceptual Computational Model of the Phosphorelay. The phosphorelay is the central pathway for integration of environmental stressors and Rap-Phr quorum signals. Environmental stressors such as starvation regulate the autophosphorylation activity of histidine kinases (KinA-E) that all interact with Spo0F. PhrA,C,E,H-derived signals modulate the phosphoryl transfer by regulating their cognate Rap-phosphatases (19–23), which dampen the phosphoryl flux by competing with Spo0B. Spo0B activates Spo0A, which is dephosphorylated by another set of aspartyl phosphatases, such as Spo0E (9). The phosphorelay is subject to a set of feedbacks exerting both positive and negative control on the concentration of phosphorylated Spo0A. At low concentrations, Spo0A~P regulates expression of phosphorelay proteins, mainly indirectly via repression of *abrB* and one of its targets *sigH* (24–26) that also up-regulates PhrC,E peptide production (27). At high (low) Spo0A~P concentrations, RapA is repressed (activated) (26). An odd topological feature is that the phosphotransferase Spo0B is the only phosphorelay step that appears to be devoid of any known feedback.

To study signal integration, we build a conceptual ordinary equation model of the phosphorelay schematically shown in Fig. 2*B* and detailed in *Methods* and in *Model Derivation* in supporting information (SI) *Appendix*. We introduce κ to represent the effective autophoshorylation rate controlled by environmental stress (equals Input κ) and π to represent the effective Rap phosphatase activity that is modulated by Phr quorum signals (equals Input π). Our model considers the steady-state concentration x of Spo0A~P as the relevant output (equals Output x) and denotes $x = f(\kappa,\pi)$ to describe the input–output relationship.

To define the conditions necessary for signal integration, we first analyzed the sensitivity of the output with respect to the input signals assuming constant protein concentrations (open-loop system, Fig. S1*A*). We find that for any system, the space of (κ, π) inputs partitions into 4 regimes (I–IV) based on whether x will respond to changes in both, one, or neither input (Fig. 2*C*, Fig. S2). The regime boundaries are defined by $\kappa_s(\pi)$ and $\pi_s(\kappa)$ that are complicated functions of the system parameters derived in *Open-Loop Model* in *SI Appendix*. In regime I, which we call the "signal integration regime," the output responds to changes in both inputs equally well. Here, the kinase activity is sufficiently low to not saturate the relay ($\kappa < \kappa_s$) and the phosphatase activity is sufficiently high ($\pi > \pi_s$) to cause a significant drain of the phosphoryl flux. In all other regimes, the output does not respond to at least one input because of insufficient phosphatase activity ($\pi < \pi_s$, regime II) or saturation of at least one

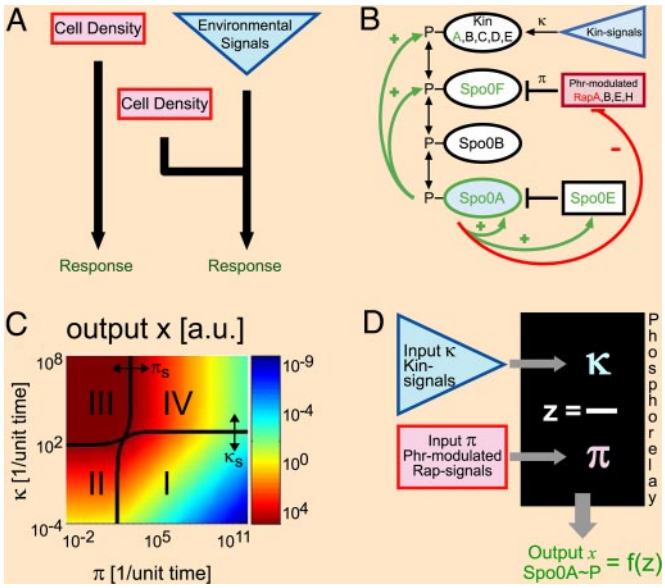

Fig. 2. Model of quorum signal integration. (*A*) In contrast to autoinducer signaling, which elicits a direct cell response (*Left*), Phr-based signals integrate with (environmental) signals (*Right*). (*B*) Schematic model of phosphorelay signaling. (*C*) Global output behavior of an open-loop phosphorelay. Only in regime I ("signal integration regime") is the output sensitive to changes in both input signals and the output responds to changes in their ratio ("ratiometric coupling"). In all other regimes (II–IV), the cell is insensitive to at least one input signal. The functions κ_s and π_s are functions of system parameters and determine the regime boundaries. (*D*) Black-box model of the phosphorelay signal integration operating as a machine to compute the quotient of the Kin-kinase κ and Phr-modulated Rap-phosphatase activity π to control the steady-state concentration of Spo0A~Px.

phosphorelay protein ($\kappa > \kappa_s$ regimes III and IV). Thus, only in regime I will the cell be able to respond to changes in both input signals simultaneously. Within regime I, the output describes diagonal isocolor lines. This implies that both signals couple such that the output depends linearly on the ratio of the input signals ("ratiometric coupling"), i.e., $f(\kappa,\pi) = f(z = \kappa/\pi) = \alpha\,\kappa/\pi$, where α is a complicated function of system parameters (Fig. 2*D*). See *Open-Loop Model* in *SI Appendix* for an analytical derivation of f.

We next show that the "low Spo0A~P" feedback architecture shown in green in Fig. 2*B* (Fig. S1*B*) expands the signal integration regime and at the same time retains the ratiometric input coupling. A typical result is shown in Fig. 3, where we find feedback (Fig. 3*B*) significantly expands the signal integration regime to larger kinase inputs compared with the open-loop system (Fig. 3*A*). A detailed study presented in *Closed loop model with low Spo0A~P feedback* in *SI Appendix* reveals that the main effect of feedback independent of its mechanisms in our model is to raise the protein concentrations, which increases the phosphoryl carrying capacity, via κ_s, before the relay saturates (Fig. S3). Unlike κ_s, feedback can either increase or decrease π_s depending on parameters. Whether feedback expands regime I depends on whether it pushes the boundary π_s between regimes I and II beyond some critical value π_*. At π_*, the phosphatase activity is strong enough to prevent activation of feedback under all circumstances. Thus, as long as feedback does not increase π_s beyond π_*, it will cause a dynamic expansion of the signal integration regime I. The exact form of f within regime I is generally dependent on the choice of transfer function to describe feedback. In general, whenever feedback operates in the x-insensitive portions of its transfer function (i.e., protein production is at either approximately basal (maximal) rate) steady-state protein and phosphorylation equations decouple, and the

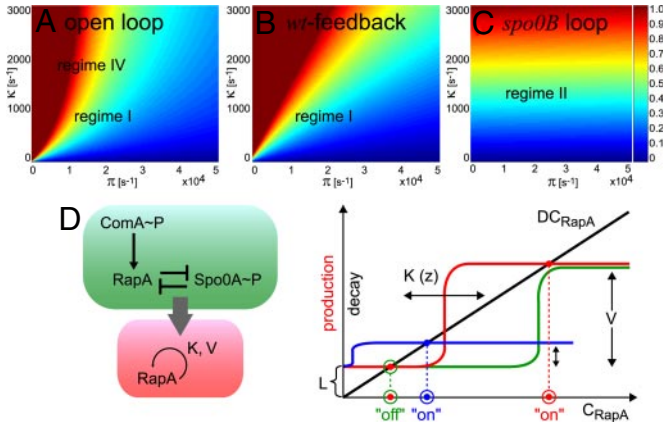

Fig. 3. Effect of feedback on signal integration (*A–C*) and RapA/PhrA expression (*D*). (*A*) Output behavior of a reference open-loop system without feedback spanning regime I and IV. (*B*) WT low Spo0A feedbacks expand the ratiometric regime I. (*C*) Adding a P_{spo0B} loop to the WT reduces severely the π sensitivity. (*D*) (*Left*) The regulatory motif of Spo0A~P and RapA cross-repression maps onto an effective autoactivating circuit for RapA production with activation coefficient *K* and maximal production *V*. (*Right*) The protein production rate as a function of Rap concentration *c* is shown for 3 different (*K*,*V*)-pairs. The protein decay rate is shown in black. In steady state, production equals decay, and the circled intersections determine the stable steady-state concentration(s) in each case. As *K* increases, RapA expression is monostable ''on'' (blue), bistable (red), and a monostable ''off'' (green). The absolute concentration of the ''on'' state is controlled by *V*, which depends on ComA activation.

system behaves identically to an open-loop system with concentrations operating at either basal (maximum) concentrations. When feedback operates in the *x*-sensitive part, *f* typically will be a more complicated function. However, numerical simulations suggest that for the most part, the ratiometric input coupling persists, and *f* describes a nonlinear function in $z = \frac{\kappa}{\pi}$. Thus, even when *f* is nonlinear in *z*, the ratiometric coupling ensures that cells will reach the same Spo0A~P level (and thus activate a downstream signal) as long as the ratio of κ and π is the same.

We next compared an in silico P_{spo0B}''mutant'' by adding an equally strong positive Spo0B feedback loop (Fig. S1*C*) to the WT system from Fig. 3*B*. The corresponding output in Fig. 3*C* describes almost horizontal iso-lines implying a severely reduced π sensitivity compared with the WT when the relay operates in the same input regime. We find that a Spo0B loop typically diminishes the dynamic expansion of the signal integration regime compared with the WT because π_s is especially sensitive to Spo0B levels (see Fig. S4 and discussion in *Effect of Spo0B feedback loop* in *SI Appendix* for details). Hence, although feedback still prevents saturation, it primarily expands the phosphatase insensitive regime II. Moreover, when the feedback transfer function is linear in *x*, the Spo0B loop destroys the ratiometric input coupling of the WT.

We therefore conclude that only within the signal integration regime is the cell susceptible to both changes in starvation ($\Delta\kappa$) as well as changes in cell density ($\Delta\pi$) simultaneously. This requires the phosphorelay to stay nonsaturated and the phosphatase activity to exceed a critical strength. Within this regime, the phosphorelay integrates both signals such that Spo0A~P levels respond to changes in their ratio, i.e.:

$$x = f(\kappa, \pi) \approx f(z) \quad \text{with} \quad z \approx \kappa/\pi. \qquad [1]$$

If we take κ to be a cellular measure of starvation conditions in the environment ($\approx$1 per food) and π an inverse measure of cell density ($\approx$1 per cell), we may interpret the control parameter *z* as (the inverse of) a ''food-per-cell'' estimate. It is plausible that certain signals need cell-density-dependent normalization to arrive at a more relevant control parameter for cellular decision making.

The phosphorelay is involved in driving the development of heterogeneous populations (14–17, 28). In our model, a potentially physiological relevant bistability arises as a result of repression of the rapA-phrA operon at high Spo0A~P levels (26). This cross-repressive feedback can be mapped into an effective autoactivating circuit for RapA/PhrA production with the effective activation coefficient *K* being a function of environmental conditions and the maximal expression level *v* that is controlled by ComA activation of the promoter (Fig. 3*D* and *Bifurcation of RapA/PhrA Expression* in *SI Appendix*). When the phosphorelay operates in the signal integration regime the bifurcation occurs as a function of the ratiometric control parameter *z* that shifts *K* and therefore alters the number of stable steady-state concentrations. For RapA we predict a monostable ''on'' state above a critical ''food per cell'' level ($K(z) < K_1$), a bistable regime at intermediate ($K_1 < K(z) < K_2$) and a monostable ''off'' below a critical level ($K(z) > K_2$). Although *z* controls the stability, the difference in expression levels between ''off'' and ''on'' is primarily modulated by ComA~P via *V*. Thus, as a population starves and *z* changes, RapA expression bifurcates, which might contribute to the level of population heterogeneity.

Experiment: Subpopulation PhrA Signaling Dynamics. The complexity of several Rap-Phr systems and kinases being involved in phosphorelay signaling will require an extended experimental study to arrive at a detailed understanding of the effective ratiometric control parameter *z*. The RapA-PhrA system is known to be heterogeneously expressed (17), suggesting that cells may even perform normalizations with respect to the size of distinct subpopulations. RapA is also strongly implied in the timing and cell fate decision making in sporulating microcolonies (28). Here, we will analyze the PhrA subpopulation signaling dynamics by means of time-lapse microscopy to follow the coordinated dynamics of RapA-PhrA expression during microcolony development, analyze the fate and physiology of the RapA-PhrA subpopulation, and qualitatively relate our results to our model predictions on RapA expression. Although our experiments will not directly address the ratiometric coupling prediction, our observations and the theoretical model will allow an interpretation of RapA-PhrA subpopulation signaling.

We first focus on RapA-PhrA expression dynamics during development of a microcolony (Fig. 4). Snapshots of a representative colony emerging from a single progenitor cell are shown in Fig. 4*A* (see Movie S1). Typical outgrowth is initially exponential for several hours. Eventually total colony area and total cell numbers stagnate, denoting entry of the colony into stationary phase $T_0 \approx 9$ h (Fig. 4*C*). The first prespores typically occur at $T_{3.5}$, that is, 3.5 h after T_0, and the vast majority of them complete mature spore development including lysis of the mother cell $\approx$10 h later. Consistent with previous observations (17), we first observe a very small, but, as predicted by our theory, across the population homogeneous, rise in P_{rapA}-driven fluorescence that varies little from basal levels. The overall still low expression may reflect only slight and very gradual activation of the promoter by ComA~P (i.e., small *V*). Coincident with T_0, we observe a clear bifurcation of the cell population into cells that strongly induce from P_{rapA} and cells that remain at low levels. The split of the population may reflect the stability change from monostable to a bistable RapA regime predicted by our model, whereas the rise in fluorescence may be a result of ComA~P activation causing the ''on'' state to shift upwards. A histogram over fluorescence intensities at $T_{4.5}$ shows a clear bimodal distribution (Fig. 4*B*). The time evolution of the distribution of fluorescence from the quorum operon is shown as a heat map in Fig. 4*D*, showing monomodal ''low'' population for $t < T_0$,

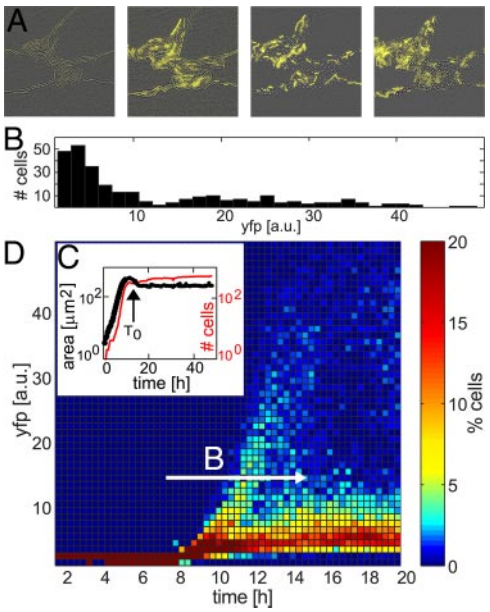

Fig. 4. Emergence of subpopulation PhrA signaling. (*A*) Snapshots of an outgrowing colony of strain *rapA/IIa* at $t \approx T_0$, T_2, T_{11}, and T_{40}. T_0 denotes entry into stationary phase. Bright-field images (gray) were overlaid with the fluorescence images derived from P_{rapA}-iyfp (yellow). (*B*) Bimodal distribution of fluorescence intensities within the cell population at $T_{4.5}$. (*C*) Log-scale growth characteristics of the colony estimated from the segmented colony area (red) and total number of segmented cells (black). (*D*) Time evolution of population frequencies with a particular YFP fluorescence intensity. A clear bifurcation into ''on'' and ''off'' cells emerges at approximately T_0.

followed by a clear emergence of a subpopulation that turns ''high'' at T_0. At later times, the intensity distribution of the high population begins to wash out (see below). The basic features of the observed population dynamics are very robust although the absolute timing and the relative proportions of the early subpopulations can vary (Fig. S5). Hence, we infer that only a subpopulation within the isogenic microcolony strongly activates PhrA peptide production at T_0 and is susceptible to it via significant transcription of the cognate Rap (Fig. S5).

We next analyzed the relationship between gene expression dynamics and cell fate by tracking the fluorescence driven by P_{rapA}-*iyfp* and P_{spoIIA}-*icfp* within the colony on the individual cell level. Successful sporulation was assigned based on the appearance of a bright prespore. Almost all cells containing a prespore completed the sporulation process and were released by lysis of the mothercell. To simplify our analysis, we split the colony population into 2 classes: (*i*) cells that completed prespore formation during the 2-day time course of the experiment (spore trajectories) and (*ii*) cells that did not (vegetative trajectories). The time evolution of YFP and CFP fluorescence is shown for a few cells in each category on the top of Fig. 5. The heat maps below represent the fluorescence intensity over time of all 294 tracked cell trajectories within the colony. We also count the number of cell divisions in each trajectory that occurred after T_0.

In Fig. 5*A*, individual trajectories are arranged from bottom to top according to the respective time t_s when the prespore became visible to allow a correlation of Rap-Phr activation with sporulation dynamics. We terminated each trajectory at its t_s. One can clearly distinguish 2 groups depending on their RapA-PhrA activation profile extracted from their YFP dynamics: (*i*) lineages executing early, rather synchronous, sporulation events that proceed without significant activation of PhrA and RapA at the bottom and, (*ii*) lineages that delayed sporulation events in which PhrA production was transiently activated at the top of the figure. At approximately T_0, early sporulators activate transcription from P_{spoIIA} nearly synchronously, giving rise to a distinct peak in the CFP signal that peaks on average ≈3.5 h before the prespore appears. Late sporulators activate PhrA (and RapA) production and, consistent with RapA's molecular function to inhibit the phosphorelay, they continue to divide, as evidenced by the increased number of cell divisions after T_0 compared with early sporulators. Ultimately when delayed sporulators activate *spoIIA* transcription, it then takes them slightly more time to complete prespore development (3.5 h for early to ≈5 h for late spores).

Fig. 5*B* shows the corresponding heat maps and cell division plots for cells that did not form a prespore during the time course of the experiment. Some cells may have activated sporulation late but had not completed prespore development. Vegetative trajectories make up ≈30% of all tracked trajectories within the colony. Within this class, we arranged the individual trajectories according to cell lineage such that daughter cell trajectories are prepended with the shared history of their mother cell. Most cells remained truly vegetative because cell divisions are observed even after 2 days. On average, cells underwent 6–7 cell divisions after T_0. Consistently, most CFP trajectories do not show the characteristic CFP peak observed for spore trajectories, whereas all trajectories activated the *rapA-phrA* operon early on and then appear to undergo repeated cycles of YFP activation and fluorescence decay. This explains the washout of the YFP on-peak of the probability density function over time in Fig. 3*B*. Further analysis reveals that the individual YFP dynamics in the vegetative cell lineages strongly correlates with the cellular length profile (Fig. S6) with an average Pearson correlation coefficient of $\langle\rho\rangle = 0.4$. We observe an increase in YFP fluorescence intensity during periods of cell elongation, followed by a decay of fluorescence intensity shortly after cell division. This could either be caused by a cell-cycle-dependent transcription dynamics or a cell-cycle-dependent variation of fluorophore stability. Fluorophore expression from a moderate constitutively activated promoter does not show the pulsatile dynamics observed for P_{rapA}-*iyfp* but a more continuous rise in fluorescence intensity over time (see Movie S2 and Fig. S7). In any case, the fluorescence dynamics observed for P_{rapA}-*iyfp*-driven fluorescence implies that the signaling PhrA peptide transcription remains active in vegetative cells long after T_0 (and its production may even be activated during periods of active cell growth only). We therefore propose that the RapA-PhrA system may allow cells to obtain a measure of the size of the actively growing subpopulation only.

Discussion

To explain the function of Phr-Rap family, different hypotheses have been put forward in the past including cell communication (5, 21), a combined form of cell density and stationary phase signaling (1), or timing of cell differentiation events on the individual cell level (29, 30). Our results suggest that key for a comprehensive understanding of their function might be to analyze their role in integrating environmental signals with (sub)population density information.

Our theoretical models show that sensitive signal integration requires kinase inputs to not saturate the relay and phosphatase signals to exceed a certain strength. Only then will cells be able to respond to both changes in starvation conditions as well as changes in cell density. Within this regime, we find that both signals couple to give rise to a single internal control parameter, the ratio of the activities, that determines the concentration of the active transcription factor Spo0A~P. Bacteria might interpret signals such as starvation, not on an absolute but rather relative basis (''food per cell''). We find that the native ''low'' Spo0A~P feedbacks typically expands the signal integration regime while retaining the ratiometric input coupling. This may allow cells to process stronger signals upon entry into stationary

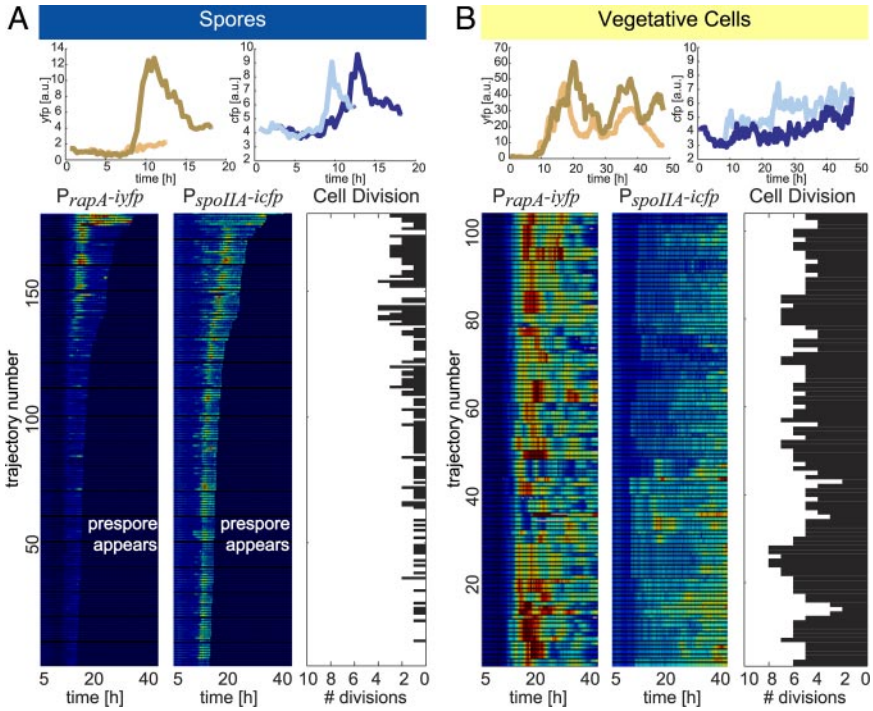

Fig. 5. Correlation between cell fate and P_{rapA}-*iyfp* and P_{spoIIA}-*icfp*-driven fluorescence for spores (*A*) and vegetative cells (*B*) within a colony. Sample trajectories within each class are shown on the top. Within each image, heat maps color code the time evolution of fluorescence intensity (red, high intensity, to blue, low intensity) for each tracked cell trajectory and relate it to the corresponding number of cell divisions after entry into stationary phase ($t > T_0$). Trajectories in *A* were arranged according to the time the prespore appeared t_s from bottom to top and in *B* clustered according to cell lineage relationship.

phase. The absence of a *spo0B* feedback might be evolved to keep the system in the signal integration regime. Intuitively, Spo0B and Rap competitively split the phosphoryl flux by binding to Spo0F. As Spo0B increases, Rap is outcompeted, desensitizing the system to changes in Rap activity. Finally we predict a bifurcation in RapA-PhrA levels as relative environmental conditions change. Although our experiments do not test the ratiometric coupling prediction, consistent with previous observations (17) and qualitative model prediction, we observe the emergence of a bimodal RapA/PhrA expression profile as the colony starves.

The complexity of several kinases and Rap/Phr systems being processed in phosphorelay signaling—that moreover may even act heterogeneously across the population—suggests a rich area of study to arrive at a more detailed understanding of the here broadly motivated "food per cell" interpretation of the ratiometric control parameter. Experimentally, we observe early rather synchronous sporulation among a majority subpopulation that involves little RapA-PhrA expression. We speculate that some other Rap-Phr system, with the constitutive RapB and its sigH up-regulated csf peptide being a likely candidate, might be involved. If this system was homogeneously expressed across the population, the initial reduction of the growing cell population could be based on an environmental measurement with respect to the total population size. Coincident with a majority population activating sporulation, we observe an up-regulation of the RapA-PhrA operon in a distinct subpopulation. Up-regulation of RapA (which may now become the dominant phosphatase) may initially delay further sporulation because PhrA must first accumulate, and this delay may serve an independent function (17, 29). However, we propose that, ultimately, decision making in the emerging RapA subpopulation may be based on normalizing environmental signals with respect to the now much smaller subpopulation of growing cells (i.e., this subpopulation is calculating "food per growing cell"). Although the ability of PhrA to mediate long-range cell–cell communication is controversial, PhrA is at least able to allow short-range intercellular signaling as the wild type is able to complement a Δ*phrA* mutant in coculture (7). In dense communities, even contact based cell-to-cell signaling might be sufficient to measure local cell counts.

For small signaling molecules that are secreted from bacteria, several functions have been proposed, including global intraspecies communication or quorum sensing (10), interspecies communication (31), diffusion sensing (32), or molecular timing devices (29). Our observation of a Rap-Phr system being expressed only in a phenotypically well-defined subpopulation may therefore be put in a broader perspective. Recent years have seen an increased appreciation of the heterogeneous population structure of monoclonal populations during stationary phase (13–16) where undomesticated strains initiate the formation of phenotypically diverse biofilms (12, 15, 18) The coordinated development of differentiated subpopulations suggests a potential need for cell–cell signaling systems that facilitate communication among and across differentiating subpopulations We thus speculate that the Rap-Phr family in *B. subtilis* represents a form of microbial cell–cell communication that constitutes an elaborate communication network that allows bacteria to integrate (environmental) signals with subpopulation structure information to drive and maintain cell differentiation in an isogenic population, similar to cell specialization during tissue development in higher organisms.

Materials and Methods

Model. In brief, the ordinary differential equation model is based on mass action kinetics for the phosphoryl-transfer reactions with forward and backward rates k_i^f, k_i^b. Effective kinase input is described by autophosphorylation with rate κ. Phosphatase reactions are modeled as effective first-order processes. Effective Rap phosphatase activity π is a function of active Rap concentration, which is controlled by the internal PEP5 concentration. The net-effective feedback in Fig. 2*B* was modeled by using Hill kinetics for protein production with maximum production v_i, activation coefficient K_i and cooperativity n. We assume nonspecific linear protein degradation/dilution (D) and

constant basal production (L_i). Heat maps in Fig. 3 were generated for $k_i^f = 300$ $nM^{-1}s^{-1}$, $k_i^b = 200$ $nM^{-1}s^{-1}$, $k_e^o = 20$ $nM^{-1}s^{-1}$, $L_i = 0.005$ nM/s, $v_i = 5.0$ nM/s, $K_i = 50$ nM, $n_i = 1$, and $D = 10^{-4}s^{-1}$.

Strains. The strain *rapA/IIA* (B168, P_{rapA}-iyfp, Cm^r, amyE::P_{spoIIA}–icfp, K_m^r) as described in ref. 27 was kindly provided by O. Kuipers (University of Groningen, The Netherlands).

Cell Culture. Sporulation was induced with a modified Sterlini–Mandelstamm protocol (33). Cells were inoculated from frozen aliquot stocks in liquid growth CH medium (GM) and grown for 2.5 h to $OD_{600} \approx 0.2$ at 37 °C. Cells were resuspended in sporulation medium (SM) supplemented with 2% GM (mod-SM). This modification results in a more robust sporulation process. Cells were diluted and transferred to a 0.5-mm mod-SM gel pad solidified with 1.5% ultrapure agarose (Invitrogen). The pad was transferred into a glass-bottom dish (Willco) and sealed with Parafilm.

Time-Lapse Microscopy. Time-lapse microscopy was performed with an Olympus IX70 equipped with Delta Vision Core (Applied Precision) and environmental temperature control (37 °C). Bright-field and fluorescence images were taken with a 100× objective (Olympus 1.40 Plan Apo) every 15–20 min and recorded with a Cool Snap HQ2 camera.

Movie Analysis. Images were analyzed with custom-written Matlab software using the *dipimage* toolbox. Segmentation uses flat-field-corrected, denoised, and contrast-enhanced bright-field images applying edge detection, intensity, and morphological operations. Spore recognition is based on intensity and size. Fluorescence intensity is averaged over the segmented objects. Lineage tracking uses object position and object overlay correspondence matching. Both segmentation and tracking results were checked manually.

ACKNOWLEDGMENTS. We thank D. Lee, Eric Battenberg, and H. Patel for help with image processing; O. Kuipers and G. Price (University of California, Berkeley, CA) for providing strains; G. Price, R. Münch, B. Lazazzera, and A. Grossman for discussions; and A. Deutschbauer, R. Skupsky, and S. Aviran for critical reading of the manuscript. This work was supported by National Institutes of Health Grant R01 GM073010-01 and by the Deutsche Forschungsgemeinschaft through fellowship BI1213-1 (to I.B.B.).

1. Pottathil M, Lazazzera BA (2003) The extracellular Phr peptide-rap phosphatase signaling circuit of *Bacillus subtilis*. *Front Biosci* 8:D32–D45.
2. Lazazzera BA, Kurtser IG, McQuade RS, Grossman AD (1999) An autoregulatory circuit affecting peptide signaling in *Bacillus subtilis*. *J Bacteriol* 181(17):5193–5200.
3. Perego M, Higgins CF, Pearce SR, Gallagher MP, Hoch JA (1991) The oligopeptide transport-system of *Bacillus-subtilis* plays a role in the initiation of sporulation. *Mol Microbiol* 5(1):173–185.
4. Rudner DZ, Ledeaux JR, Ireton K, Grossman AD (1991) The Spo0K locus of *Bacillus-subtilis* is homologous to the oligopeptide permease locus and is required for sporulation and competence. *J Bacteriol* 173(4):1388–1398.
5. Lazazzera BA, Solomon JM, Grossman AD (1997) An exported peptide functions intracellularly to contribute to cell density signaling in *B-subtilis*. *Cell* 89(6):917–925.
6. Lazazzera BA, Grossman AD (1998) The ins and outs of peptide signaling. *Trends Microbiol* 6(7):288–294.
7. Perego M, Hoch JA (1996) Cell–cell communication regulates the effects of protein aspartate phosphatases on the phosphorelay controlling development in *Bacillus subtilis*. *Proc Natl Acad Sci USA* 93(4):1549–1553.
8. Solomon JM, Lazazzera BA, Grossman AD (1996) Purification and characterization of an extracellular peptide factor that affects two different developmental pathways in *Bacillus subtilis*. *Genes Dev* 10(16):2014–2024.
9. Burbulys D, Trach KA, Hoch JA (1991) Initiation of sporulation in *Bacillus-subtilis* is controlled by a multicomponent phosphorelay. *Cell* 64(3):545–552.
10. Miller MB, Bassler BL (2001) Quorum sensing in bacteria. *Annu Rev Microbiol* 55: 165–199.
11. Grossman AD, Losick R (1988) Extracellular control of spore formation in *Bacillus subtilis*. *Proc Natl Acad Sci USA* 85(12):4369–4373.
12. Vlamakis H, Aguilar C, Losick R, Kolter R (2008) Control of cell fate by the formation of an architecturally complex bacterial community. *Genes Dev* 22(7):945–953.
13. Dubnau D, Losick R (2006) Bistability in bacteria. *Mol Microbiol* 61(3):564–572.
14. Smits WK, Kuipers OP, Veening JW (2006) Phenotypic variation in bacteria:The role of feedback regulation. *Nat Rev Microbiol* 4(4):259–271.
15. Chai YR, Chu F, Kolter R, Losick R (2008) Bistability and biofilm formation in *Bacillus subtilis*. *Mol Microbiol* 67:254–263.
16. Veening JW, et al. (2008) Transient heterogeneity in extracellular protease production by *Bacillus subtilis*. *Mol Syst Biol* 4:186.
17. Veening JW, Hamoen LW, Kuipers OP (2005) Phosphatases modulate the bistable sporulation gene expression pattern in *Bacillus subtilis*. *Mol Microbiol* 56(6):1481–1494.
18. Branda SS, Gonzalez-Pastor JE, Ben-Yehuda S, Losick R, Kolter R (2001) Fruiting body formation by *Bacillus subtilis*. *Proc Natl Acad Sci USA* 98(20):11621–11626.
19. Mueller JP, Sonenshein AL (1992) Role of the *Bacillus-subtilis* GsiA gene in regulation of early sporulation gene-expression. *J Bacteriol* 174(13):4374–4383.
20. Perego M, et al. (1994) Multiple protein aspartate phosphatases provide a mechanism for the integration of diverse signals in the control of development in *Bacillus-subtilis*. *Cell* 79(6):1047–1055.
21. Perego M, Hoch JA (1996) Protein aspartate phosphatases control the output of two-component signal transduction systems. *Trends Genet* 12(3):97–101.
22. Jiang M, Grau R, Perego M (2000) Differential processing of propeptide inhibitors of Rap phosphatases in *Bacillus subtilis*. *J Bacteriol* 182(2):303–310.
23. Smits WK, et al. (2007) Temporal separation of distinct differentiation pathways by a dual specificity Rap-Phr system in *Bacillus subtilis*. *Mol Microbiol* 65(1):103–120.
24. Weir J, Predich M, Dubnau E, Nair G, Smith I (1991) Regulation of Spo0H, a gene coding for the *Bacillus-subtilis* sigma-H factor. *J Bacteriol* 173(2):521–529.
25. Predich M, Nair G, Smith I (1992) *Bacillus-subtilis* early sporulation genes KinA, Spo0F, and Spo0A are transcribed by the RNA-polymerase containing sigma-H. *J Bacteriol* 174(9):2771–2778.
26. Fujita M, Gonzalez-Pastor JE, Losick R (2005) High and low threshold genes in the Spo0A regulon of *Bacillus subtilis*. *J Bacteriol* 187(4):1357–1368.
27. McQuade RS, Comella N, Grossman AD (2001) Control of a family of phosphatase regulatory genes (phr) by the alternate sigma factor sigma-H of *Bacillus subtilis*. *J Bacteriol* 183(16):4905–4909.
28. Veening JW, et al. (2008) Bet-hedging and epigenetic inheritance in bacterial cell development. *Proc Natl Acad Sci USA* 105(11):4393–4398.
29. Perego M (1997) A peptide export–import control circuit modulating bacterial development regulates protein phosphatases of the phosphorelay. *Proc Natl Acad Sci USA* 94(16):8612–8617.
30. Perego M, Brannigan JA (2001) Pentapeptide regulation of aspartyl-phosphate phosphatases. *Peptides* 22(10):1541–1547.
31. Federle MJ, Bassler BL (2003) Interspecies communication in bacteria. *J Clin Invest* 112(9):1291–1299.
32. Redfield RJ (2002) Is quorum sensing a side effect of diffusion sensing? *Trends Microbiol* 10(8):365–370.
33. Harwood CR and Cutting SM (1990) *Molecular Biological Methods for Bacillus* (Wiley, New York) pp 396–399.